Journal of Science and Technology in Civil Engineering, NUCE 2020. 14 (3): 136–150

FREE VIBRATION OF BIDIRECTIONAL FUNCTIONALLY GRADED SANDWICH BEAMS USING A FIRST-ORDER SHEAR DEFORMATION FINITE ELEMENT FORMULATION

Le Thi Ngoc Anh[a,b,*], Vu Thi An Ninh[c], Tran Van Lang[a,b], Nguyen Dinh Kien[b,d]

[a]*Institute of Applied Mechanics and Informatics, VAST, 291 Dien Bien Phu street, Ho Chi Minh city, Vietnam*
[b]*Graduate University of Science and Technology, VAST, 18 Hoang Quoc Viet street, Hanoi, Vietnam*
[c]*University of Transport and Communications, 3 Cau Giay street, Dong Da district, Hanoi, Vietnam*
[d]*Institute of Mechanics, VAST, 18 Hoang Quoc Viet, Hanoi, Vietnam*

Article history:
Received 06/7/2020, Revised 09/8/2020, Accepted 10/8/2020

Abstract

Free vibration of bidirectional functionally graded sandwich (BFGSW) beams is studied by using a first-order shear deformation finite element formulation. The beams consist of three layers, a homogeneous core and two functionally graded skin layers with material properties varying in both the longitudinal and thickness directions by power gradation laws. The finite element formulation with the stiffness and mass matrices evaluated explicitly is efficient, and it is capable of giving accurate frequencies by using a small number of elements. Vibration characteristics are evaluated for the beams with various boundary conditions. The effects of the power-law indexes, the layer thickness ratio, and the aspect ratio on the frequencies are investigated in detail and highlighted. The influence of the aspect ratio on the frequencies is also examined and discussed.

Keywords:
BFGSW beam; first-order shear deformation theory; free vibration; finite element method.

https://doi.org/10.31814/stce.nuce2020-14(3)-12

1. Introduction

With the development in the manufacturing methods [1, 2], functionally graded materials (FGMs) can be incorporated in the sandwich construction to improve the performance of the structural components. The functionally graded sandwich (FGSW) structures can be designed to have a smooth variation of material properties among layer interfaces, which helps to eliminate the interface separation of the conventional sandwich structures. Many investigations on mechanical vibration of FGSW structures have been reported in the literature, contributions that are most relevant to the present work are discussed below.

Amirani et al. [3] studied free vibration of FGSW beam with a functionally graded core with the aid of the element free Galerkin method. Based on Reddy-Birkford shear deformation theory, Vo et al. [4] presented a finite element model for free vibration and buckling analyses of FGSW beams. In [5], the thickness stretching effect was included in the shear deformation theory in the

*Corresponding author. *E-mail address:* lengocanhkhtn@gmail.com (Anh, L. T. N.)

analysis of FGSW beams. A hyperbolic shear deformation beam theory was used by Bennai et al. [6] to study free vibration and buckling of FGSW beams. Trinh et al. [7] evaluated the fundamental frequency of FGSW beams by using the state space approach. The modified Fourier series method was adopted by Su et al. [8] to study free vibration of FGSW beams resting on a Pasternak foundation. The authors used both the Voigt and Mori-Tanaka models to estimate the effective material properties of the beams. A finite element formulation based on hierarchical displacement field was derived by Mashat et al. [9] for evaluating natural frequencies of laminated and sandwich beams. The accuracy and efficiency of the formulation were shown through the numerical investigation. Şimşek and Alshujairi [10] investigated bending and vibration of FGSW beams using a semi-analytical method. Based on various shear deformation theories, Dang and Huong [11] studied free vibration of FGSW beams with a FGM porous core and FGM faces resting on Winkler foundation. Navier's solution has been used by the authors for obtaining frequencies of the beams.

The FGM beams discussed in the above references, however, have material properties varying in the thickness direction only. These unidirectional FGM beams are not efficient to withstand the multidirectional loadings. The bidirectional FGM beam models with the volume fraction of constituents varying in both the thickness and longitudinal directions have been proposed and their mechanical behaviour was investigated recently. Şimşek [12] studied vibration of Timoshenko beam under moving forces by considering the material properties varying in both the length and thickness directions by an exponential function. Free vibration analysis of bidirectional FGM beams was investigated by Karamanli [13] using a third-order shear deformation. Hao and Wei [14] assumed an exponential variation for the material properties in both the thickness and length directions in vibration analysis of FGM beams. Nguyen et al. [15] studied forced vibration of Timoshenko beams under a moving load, in which the beam model is assumed to be formed from four different materials with material properties varying in both the thickness and longitudinal directions by power-law functions. A finite element formulation was derived by the authors to compute the dynamic response of the beams. Nguyen and Tran [16, 17] studied free vibration of bidirectional FGM beams using the shear deformable finite element formulations. The effects of longitudinal variation of cross-section and temperature rise have been taken into consideration in [16, 17], respectively.

In this paper, free vibration of bidirectional functionally graded sandwich (BFGSW) beams is studied by using a finite element formulation. The beams made from three distinct materials are composed of three layers, a homogeneous core and two bidirectional FGM face layers with material properties varying in both the thickness and longitudinal directions by power gradation laws. Based on the first-order shear deformation theory, a finite element formulation is derived and employed to compute the vibration characteristics of the beams with various boundary conditions. The accuracy of the derived formulation is validated by comparing obtained results with those in the references. A parametric study is carried out to show the effects of the material indexes, the layer thickness and aspect ratios on the vibration behaviour of the beams.

2. Mathematical formulation

A BFGSW beam with length L, rectangular cross-section ($b \times h$) as illustrated in Fig. 1 is considered. The beam is assumed to be made from three materials, material 1 (M1), material 2 (M2), and material 3 (M3). The beam consists of three layers, a homogenous core of M1 and two BFGM skin layers of M1, M2, and M3. Denote z_0, z_1, z_2, z_3, in which $z_0 = -h/2, z_3 = h/2$, as the vertical coordinates of the bottom surface, interfaces, and top face, respectively.

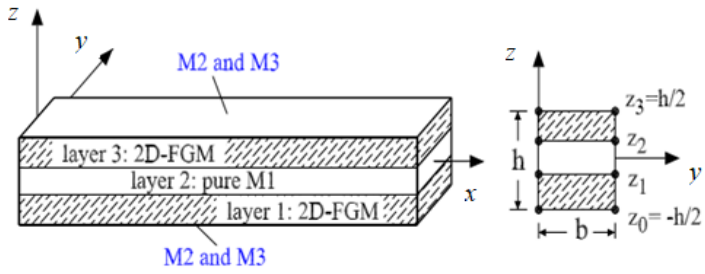

Figure 1. The BFGSW Beam model

The volume fractions of M1, M2 and M3 are assumed to vary in the x and z directions according to

$$
\begin{aligned}
&\text{for} \quad z \in [z_0, z_1] \quad \begin{cases} V_1^{(1)} = \left(\dfrac{z - z_0}{z_1 - z_0}\right)^{n_z} \\ V_2^{(1)} = \left[1 - \left(\dfrac{z - z_0}{z_1 - z_0}\right)^{n_z}\right]\left[1 - \left(\dfrac{x}{L}\right)^{n_x}\right] \\ V_3^{(1)} = \left[1 - \left(\dfrac{z - z_0}{z_1 - z_0}\right)^{n_z}\right]\left(\dfrac{x}{L}\right)^{n_x} \end{cases} \\
&\text{for} \quad z \in [z_1, z_2] \quad V_1^{(2)} = 1, V_2^{(2)} = V_3^{(2)} = 0 \\
&\text{for} \quad z \in [z_2, z_3] \quad \begin{cases} V_1^{(3)} = \left(\dfrac{z - z_3}{z_2 - z_3}\right)^{n_z} \\ V_2^{(3)} = \left[1 - \left(\dfrac{z - z_3}{z_2 - z_3}\right)^{n_z}\right]\left[1 - \left(\dfrac{x}{L}\right)^{n_x}\right] \\ V_3^{(3)} = \left[1 - \left(\dfrac{z - z_3}{z_2 - z_3}\right)^{n_z}\right]\left(\dfrac{x}{L}\right)^{n_x} \end{cases}
\end{aligned} \tag{1}
$$

where V_1, V_2, and V_3 are, respectively, the volume fraction of the M1, M2, and M3; n_x and n_z are the material grading indexes, defining the variation of the constituents in the x and z directions, respectively. The model defines a softcore sandwich beam if M1 is a metal and a hardcore one if M1 is a ceramic. The variations of the volume fractions V_1, V_2, and V_3 in the thickness and length directions are illustrated in Fig. 2 for $n_x = n_z = 0.5$, and $z_1 = -h/6, z_2 = h/6$.

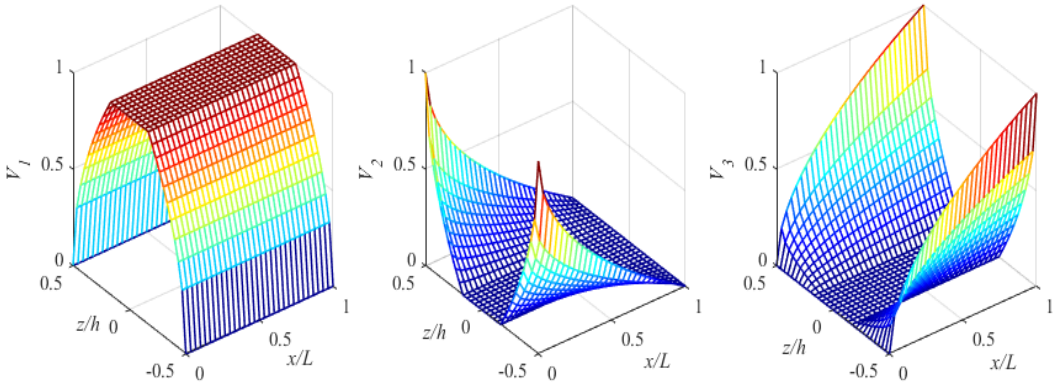

Figure 2. Variation of the volume fractions V_1, V_2, and V_3 of BFGSW beam for $n_x = n_z = 0.5, z_1 = -h/6, z = h/6$

The effective properties $P_f^{(k)}$ of the k^{th} layer ($k = 1:3$) evaluated by Voigt's model are of the form

$$P_f^{(k)} = P_1 V_1^{(k)} + P_2 V_2^{(k)} + P_3 V_3^{(k)} \tag{2}$$

where P_1, P_2, and P_3 are the properties such as elastic moduli and mass density of M1, M2, and M3, respectively

$$\begin{cases} P_f^{(1)}(x,z) = [P_1 - P_{23}(x)]\left(\dfrac{z-z_0}{z_1-z_0}\right)^{n_z} + P_{23}(x) & \text{for } z \in [z_0, z_1] \\ P_f^{(2)}(x,z) = P_1 & \text{for } z \in [z_1, z_2] \\ P_f^{(3)}(x,z) = [P_1 - P_{23}(x)]\left(\dfrac{z-z_3}{z_2-z_3}\right)^{n_z} + P_{23}(x) & \text{for } z \in [z_2, z_3] \end{cases} \tag{3}$$

where

$$P_{23}(x) = P_2 - (P_2 - P_3)\left(\frac{x}{L}\right)^{n_x} \tag{4}$$

Based on the first-order shear deformation theory, the displacements in the x and z directions, $u(x,z,t)$ and $w(x,z,t)$ are given by

$$u(x,z,t) = u_0(x,t) - z\theta; \quad w(x,z,t) = w_0(x,t) \tag{5}$$

where $u_0(x,t), w_0(x,t)$ are, respectively, the axial and transverse displacements of a point on the x-axis; t is the time variable, and θ is the cross-sectional rotation.

The axial strain and shear strain resulted from Eq. (5) are

$$\begin{aligned} \varepsilon_{xx} &= u_{0,x} - z\theta_{,x} \\ \gamma_{xz} &= w_{0,x} - \theta \end{aligned} \tag{6}$$

Based on the Hooke's law, the axial and shear stresses, σ_{xx} and τ_{xz}, are of the form

$$\begin{Bmatrix} \sigma_{xx} \\ \tau_{xz} \end{Bmatrix} = \begin{bmatrix} E_f^{(k)}(x,z) & 0 \\ 0 & \psi G_f^{(k)}(x,z) \end{bmatrix} \begin{Bmatrix} \varepsilon_{xx} \\ \gamma_{xz} \end{Bmatrix} \tag{7}$$

where σ_{xx} and τ_{xz} are, respectively, the axial and shear stresses, $E_f^{(k)}$, $G_f^{(k)}$ are the effective Young and shear moduli, given by Eq. (3); ψ is the shear correction factor, chosen by 5/6 for the beam with the rectangular cross-section.

The strain energy (U) of the FGSW beam is then given by

$$\begin{aligned} U &= \frac{1}{2}\int_0^L \int_A (\sigma_{xx}\varepsilon_{xx} + \gamma_{zx}\tau_{xz}) dA dx \\ &= \frac{1}{2}\int_0^L \left[A_{11}u_{0,x}^2 - 2A_{12}u_{0,x}\theta_{,x} + A_{22}\theta_{,x}^2 + \psi A_{33}(w_{0,x} - \theta)^2\right] dx \end{aligned} \tag{8}$$

where $A = bh$ is the cross-sectional area; A_{11}, A_{12}, A_{22}, and A_{33} are, respectively, the extensional, extensional-bending coupling, bending, and shear rigidities, defined as

$$\begin{aligned}(A_{11}, A_{12}, A_{22}) &= b\sum_{k=1}^{3}\int_{z_{k-1}}^{z_k} E_f^{(k)}(x,z)\left(1, z, z^2\right)dz \\ A_{33} &= b\sum_{k=1}^{3}\int_{z_{k-1}}^{z_k} G_f^{(k)}(x,z)dz\end{aligned} \tag{9}$$

Substituting $E_f^{(k)}$ and $G_f^{(k)}$ from Eq. (3) into (9), one can write the rigidities in the form

$$A_{ij} = A_{ij}^{M1} + A_{ij}^{M2} + A_{ij}^{M1M2} + A_{ij}^{M2M3}\left(\frac{x}{L}\right)^{n_x}, \quad (i, j = 1, ..., 3) \tag{10}$$

where $A_{ij}^{M1}, A_{ij}^{M2}, A_{ij}^{M1M2}$, and A_{ij}^{M2M3} are, respectively, the rigidities contributed from M1, M2, and M3, and their couplings of the FGM beam with the material properties varying in the thickness direction only. These terms can be explicitly evaluated, and their expressions are given by Eqs. (A.1) to (A.4) in Appendix A.

The kinetic energy resulted from Eq. (5) is of the form

$$T = \frac{1}{2}\int_0^L\int_V \rho_f^{(k)}(x,z)\left(\dot{u}^2 + \dot{w}^2\right)dAdx = \frac{1}{2}\int_0^L\left[I_{11}\left(\dot{u}_0^2 + \dot{w}_0^2\right) - 2I_{12}\dot{u}_0\dot{\theta} + I_{22}\dot{\theta}^2\right]dx \tag{11}$$

where an over is used to denote the derivative with respect to time variable t and $\rho_f^{(k)}$ is the mass density. I_{11}, I_{12}, I_{22} are the mass moments, defined as

$$(I_{11}, I_{12}, I_{22}) = b\sum_{k=1}^{3}\int_{z_{k-1}}^{z_k}\rho_f^{(k)}(x,z)\left(1, z, z^2\right)dz \tag{12}$$

As the rigidities, the above mass moments can also be written in the form

$$I_{ij} = I_{ij}^{M1} + I_{ij}^{M2} + I_{ij}^{M1M2} + I_{ij}^{M2M3}\left(\frac{x}{L}\right)^{n_x}, \quad (i, j = 1, ..., 3) \tag{13}$$

where $I_{ij}^{M1}, I_{ij}^{M2}, I_{ij}^{M1M2}, I_{ij}^{M2M3}$ are given by Eqs. (A.5)–(A.7) in Appendix A.

3. Finite element formulation

Assume that the beam is being divided into *nELE* elements with length of l. The vector of nodal displacements for a two-node generic beam element, (i, j), contains six components as

$$\mathbf{d} = \left\{\begin{array}{cccccc} u_i & w_i & \theta_i & u_j & w_j & \theta_j \end{array}\right\}^T \tag{14}$$

where u_i, w_i, and θ_i are the values of u_0, w_0, and θ at the node i; u_j, w_j, and θ_j are the corresponding values of these quantities at the node j. The superscript "T" in Eq. (14) and hereafter is used to indicate the transpose of a vector or a matrix.

The displacements $u_0(x,t)$, $w_0(x,t)$ and the rotation $\theta(x,t)$ are interpolated as

$$u_0 = \mathbf{N}_u^T \mathbf{d}; \quad w_0 = \mathbf{N}_w^T \mathbf{d}; \quad \theta = \mathbf{N}_\theta^T \mathbf{d} \tag{15}$$

where $\mathbf{N}_u = \{N_{u1}, N_{u2}\}$, $\mathbf{N}_w = \{N_{w1}, N_{w2}, N_{w3}, N_{w4}\}$, and $\mathbf{N}_\theta = \{N_{\theta1}, N_{\theta2}, N_{\theta3}, N_{\theta4}\}$ are the matrices of interpolating functions for u_0, w_0, and θ herein. The following polynomials are adopted in the present work.

- Axial displacement u_0

$$N_{u1} = \frac{x}{l}; \quad N_{u2} = 1 - \frac{x}{l} \tag{16}$$

- Transverse displacement w_0

$$\begin{aligned}
N_{w1} &= \frac{1}{(1+\lambda)}\left[2\left(\frac{x}{l}\right)^3 - 3\left(\frac{x}{l}\right)^2 - \lambda\left(\frac{x}{l}\right) + (1+\lambda)\right] \\
N_{w2} &= \frac{1}{(1+\lambda)}\left[\left(\frac{x}{l}\right)^3 - \left(2+\frac{\lambda}{2}\right)\left(\frac{x}{l}\right)^2 + \left(1+\frac{\lambda}{2}\right)\left(\frac{x}{l}\right)\right] \\
N_{w3} &= \frac{1}{(1+\lambda)}\left[2\left(\frac{x}{l}\right)^3 - 3\left(\frac{x}{l}\right)^2 - \frac{\lambda}{2}\left(\frac{x}{l}\right)\right] \\
N_{w2} &= \frac{1}{(1+\lambda)}\left[\left(\frac{x}{l}\right)^3 - \left(1-\frac{\lambda}{2}\right)\left(\frac{x}{l}\right)^2 - \frac{\lambda}{2}\left(\frac{x}{l}\right)\right]
\end{aligned} \tag{17}$$

- Rotation θ

$$\begin{aligned}
N_{\theta1} &= \frac{6}{(1+\lambda)\,l}\left[\left(\frac{x}{l}\right)^2 - \left(\frac{x}{l}\right)\right]; \quad N_{\theta2} = -\frac{1}{(1+\lambda)}\left[3\left(\frac{x}{l}\right)^2 - (4+\lambda)\left(\frac{x}{l}\right) + (1+\lambda)\right] \\
N_{\theta3} &= -\frac{6}{(1+\lambda)\,l}\left[\left(\frac{x}{l}\right)^2 - \left(\frac{x}{l}\right)\right]; \quad N_{\theta4} = \frac{1}{(1+\lambda)}\left[3\left(\frac{x}{l}\right)^2 - (2+\lambda)\left(\frac{x}{l}\right)\right]
\end{aligned} \tag{18}$$

where $\lambda = 12A_{22}/\left(l^2 \psi A_{33}\right)$. The cubic and quadratic polynomials in Eqs. (17) and (18) were derived by Kosmatka [18], and have been employed by several authors to formulate finite element formulations for analysis of FGM beams, e.g. Shahba et al. [19], Nguyen et al. [15].

Based on Eq. (14), one can write the strain and kinetic energies in Eqs. (8) and (11) in the forms

$$U = \frac{1}{2}\sum_{i=1}^{nELE} \mathbf{d}^T \mathbf{k} \mathbf{d}; \quad T = \frac{1}{2}\sum_{i=1}^{nELE} \dot{\mathbf{d}}^T \mathbf{m} \dot{\mathbf{d}} \tag{19}$$

with the element stiffness and mass matrices $\mathbf{k}$ and $\mathbf{m}$ can be written in the forms

$$\mathbf{k} = \mathbf{k}_{11} + \mathbf{k}_{12} + \mathbf{k}_{22} + \mathbf{k}_{33} \tag{20}$$

$$\mathbf{m} = \mathbf{m}_{11} + \mathbf{m}_{12} + \mathbf{m}_{22} \tag{21}$$

where

$$\begin{aligned}
\mathbf{k}_{11} &= \int_0^l \mathbf{N}_{u,x}^T A_{11} \mathbf{N}_{u,x} dx; \quad \mathbf{k}_{12} = -\int_0^l \mathbf{N}_{u,x}^T A_{12} \mathbf{N}_{\theta,x} dx \\
\mathbf{k}_{22} &= \int_0^l \mathbf{N}_{\theta,x}{}^T A_{22} \mathbf{N}_{\theta,x} dx; \quad \mathbf{k}_{33} = \int_0^l \left(\mathbf{N}_{w,x} - \mathbf{N}_\theta\right)^T \psi A_{33} \left(\mathbf{N}_{w,x} - \mathbf{N}_\theta\right) dx
\end{aligned} \tag{22}$$

and

$$\mathbf{m}_{11} = \int_0^l \left(N_u^T I_{11} N_u + N_w^T I_{11} N_w\right) dx; \quad \mathbf{m}_{12} = -\int_0^l N_u^T I_{12} N_\theta dx; \quad \mathbf{m}_{22} = \int_0^l {N_\theta}^T I_{22} N_\theta dx \tag{23}$$

The equations of motion for the beam in the discrete form is as follows

$$\mathbf{M}\ddot{\mathbf{D}} + \mathbf{K}\mathbf{D} = \mathbf{0} \tag{24}$$

where $\mathbf{D}$, $\ddot{\mathbf{D}}$, $\mathbf{M}$ and $\mathbf{K}$ are, respectively, the structural vectors of nodal displacements and accelerations, mass, and stiffness matrices. Assuming a harmonic form for vector of nodal displacements, Eq. (24) leads to an eigenvalue problem for determining the frequency ω as

$$\left(\mathbf{K} - \omega^2 \mathbf{M}\right) \bar{\mathbf{D}} = \mathbf{0} \tag{25}$$

where ω is the circular frequency and $\bar{\mathbf{D}}$ is the vibration amplitude. Eq. (14) leads to an eigenvalue problem, and its solution can be obtained by the standard method.

4. Numerical results

In this section, a soft core BFGSW beam made from aluminum (Al), zirconia (ZrO_2), and alumina (Al_2O_3) (as M1, M2, and M3, respectively) with the material properties of these constituent materials listed in Table 1 is employed in the numerical investigation. Three types of boundary conditions, namely simply supported (SS), clamped-clamped (CC), and clamped-free (CF) are considered.

Table 1. Properties of constituent materials of BFGSW beam

Materials	Note	E (GPa)	ρ (kg/m^3)	v
Alumina	M1	380	3960	0.3
ZrO_2	M2	150	3000	0.3
Aluminum	M3	70	2702	0.3

The non-dimensional frequency in this work is defined according to [4] as

$$\mu_i = \frac{\omega_i L^2}{h}\sqrt{\frac{\rho_{Al}}{E_{Al}}} \tag{26}$$

where ω_i is the ith natural frequency. Three numbers in the brackets as introduced in Ref. [4, 5] are used herein to denote the layer thickness ratio, e.g. (1-2-1) means that the thickness ratio of the layers from bottom to top surfaces is 1:2:1.

Before computing the vibration characteristics of BFGSW beams, the accuracy of the derived formulation needs to be verified. Since there is no data on the frequencies of the present beam available in the literature, the verification is carried for a special case of a unidirectional FGSW beam. Since Eq. (1) results in $V_2 = 0$ when $n_x = 0$, and in this case the BFGSW beam becomes a unidirectional FGSW beam formed from M1 and M3 with material properties varying in the thickness direction only. Thus, the frequencies of the unidirectional FGSW beam can be obtained from the present formulation by simply setting n_x to zero. Table 2 compares the fundamental frequency of the unidirectional FGSW

Table 2. Comparison of dimensionless fundamental frequencies for unidirectional FGM sandwich beam

n_z	Source	(1-0-1)	(2-1-2)	(1-1-1)	(2-2-1)	(1-2-1)	(1-8-1)
0.5	Ref. [4]	4.8579	4.7460	4.6294	4.4611	4.4160	3.7255
	Present	4.8646	4.7545	4.6390	4.4689	4.4248	3.7282
1	Ref. [4]	5.2990	5.2217	5.1160	4.9121	4.8938	4.0648
	Present	5.3061	5.2325	5.1296	4.9232	4.9080	4.0702
2	Ref. [4]	5.5239	5.5113	5.4410	5.2242	5.2445	4.3542
	Present	5.5293	5.5218	5.4559	5.2365	5.2627	4.3627
5	Ref. [4]	5.5645	5.6382	5.6242	5.4166	5.4843	4.5991
	Present	5.5672	5.6462	5.6375	5.4278	5.5038	4.6109
10	Ref. [4]	5.5302	5.6382	5.6621	5.4667	5.5575	4.6960
	Present	5.5316	5.6414	5.6738	5.4766	5.5765	4.7094

beam with $L/h = 20$ obtained in the present work with that of Ref. [4] for various values of the layer thickness ratio. Very good agreement between the result of the present work with that of Ref. [4] is noted from Table 2.

Table 3 shows the convergence of the derived formulation in evaluating the fundamental frequency parameter of the BFGSW beam. As seen from the table, the convergence is achieved by using 26 elements, regardless of the material indexes and the thickness ratio. In this regard, 26 elements are used in all the computations reported below.

Table 3. Convergence of the formulation in evaluating frequencies of BFGSW beam

$(h_1 : h_2 : h_3)$	n_x	n_z	$nELE = 16$	$nELE = 18$	$nELE = 20$	$nELE = 22$	$nELE = 24$	$nELE = 26$
(2-1-2)	0.5	1/3	4.0588	4.0587	4.0586	4.0585	4.0585	4.0585
		1	4.8336	4.8334	4.8333	4.8331	4.8330	4.8330
		3	5.1781	5.1779	5.1778	5.1777	5.1776	5.1776
	1	1/3	3.8594	3.8593	3.8592	3.8592	3.8592	3.8592
		1	4.5370	4.5368	4.5367	4.5366	4.5365	4.5365
		3	4.8517	4.8515	4.8514	4.8513	4.8511	4.8511
(2-2-1)	0.5	1/3	3.8588	3.8587	3.8586	3.8585	3.8585	3.8585
		1	4.5648	4.5646	4.5645	4.5643	4.5642	4.5642
		3	4.9436	4.9434	4.9432	4.9430	4.9429	4.9429
	1	1/3	3.6905	3.6904	3.6903	3.6902	3.6902	3.6902
		1	4.3028	4.3027	4.3025	4.3024	4.3023	4.3023
		3	4.6407	4.6405	4.6403	4.6402	4.6401	4.6401

To investigate the effects of the material grading indexes and the layer thickness ratio on the fundamental frequencies, different types of symmetric and non-symmetric BFGSW beam with various boundary conditions are considered. The numerical results of fundamental frequency parameters of the BFGSW beam with an aspect ratio $L/h = 20$ are given in Tables 4, 5, and 6 for the SS, CC, and CF beams, respectively. As seen from the tables, the frequency parameter increases by increasing the index n_z, but it decreases by the increase of the n_x, irrespective of the layer thickness ratio and the boundary condition. An increase of frequencies by the increase of the index n_z can be explained by the change of the effective Young's modulus as shown by Eqs. (1) and (3). When index n_z increases,

Table 4. Fundamental frequency parameters of SS beam with $L/h = 20$ for various grading indexes and layer thickness ratios

n_x	n_z	(1-0-1)	(2-1-2)	(2-1-1)	(1-1-1)	(2-2-1)	(1-2-1)	(1-8-1)
1/3	0	2.8371	2.8371	2.8371	2.8371	2.8371	2.8371	2.8371
	1/3	4.2644	4.1609	4.0616	4.0627	3.9452	3.8946	3.3997
	0.5	4.6413	4.5371	4.4106	4.4294	4.2789	4.2334	3.6104
	1	5.0560	4.9807	4.8278	4.8811	4.6957	4.6736	3.9137
	2	5.2742	5.2562	5.0967	5.1877	4.9881	5.0017	4.1756
	5	5.3221	5.3818	5.2365	5.3639	5.1705	5.2287	4.3998
0.5	0	2.8371	2.8371	2.8371	2.8371	2.8371	2.8371	2.8371
	1/3	4.1562	4.0584	3.9673	3.9663	3.8584	3.8093	3.3516
	0.5	4.5119	4.4119	4.2951	4.3097	4.1708	4.1253	3.5457
	1	4.9079	4.8328	4.6903	4.7365	4.5640	4.5388	3.8266
	2	5.1208	5.0980	4.9480	5.0295	4.8423	4.8496	4.0705
	5	5.1728	5.2224	5.0847	5.2005	5.0180	5.0668	4.2801
1	0	2.8371	2.8371	2.8371	2.8371	2.8371	2.8371	2.8371
	1/3	3.9446	3.8591	3.7838	3.7796	3.6902	3.6454	3.2606
	0.5	4.2549	4.1649	4.0674	4.0749	3.9588	3.9149	3.4227
	1	4.6086	4.5363	4.4152	4.4484	4.3022	4.2726	3.6593
	2	4.8062	4.7766	4.6470	4.7102	4.5494	4.5460	3.8667
	5	4.8634	4.8954	4.7744	4.8679	4.7087	4.7405	4.0464
5	0	2.8371	2.8371	2.8371	2.8371	2.8371	2.8371	2.8371
	1/3	3.4621	3.4076	3.3665	3.3587	3.3095	3.2785	3.0601
	0.5	3.6597	3.5980	3.5429	3.5394	3.4736	3.4391	3.1500
	1	3.8999	3.8425	3.7705	3.7797	3.6933	3.6621	3.2854
	2	4.0476	4.0120	3.9314	3.9583	3.8595	3.8409	3.4080
	5	4.1053	4.1061	4.0272	4.0740	3.9725	3.9742	3.5172

Table 5. Fundamental frequency parameters of CC beam with $L/h = 20$ for various grading indexes and layer thickness ratios

n_x	n_z	(1-0-1)	(2-1-2)	(2-1-1)	(1-1-1)	(2-2-1)	(1-2-1)	(1-8-1)
1/3	0	6.3496	6.3496	6.3496	6.3496	6.3496	6.3496	6.3496
	1/3	9.3196	9.0997	8.8966	8.8931	8.6518	8.5415	7.5147
	0.5	10.1077	9.8836	9.6252	9.6555	9.3469	9.2443	7.9501
	1	10.9797	10.8123	10.4993	10.5981	10.2180	10.1592	8.5770
	2	11.4450	11.3945	11.0668	11.2425	10.8322	10.8444	9.1188
	5	11.5559	11.6664	11.3665	11.6179	11.2191	11.3221	9.5832
0.5	0	6.3496	6.3496	6.3496	6.3496	6.3496	6.3496	6.3496
	1/3	9.0837	8.8777	8.6919	8.6855	8.4645	8.3596	7.4142
	0.5	9.8209	9.6084	9.3709	9.3941	9.1104	9.0104	7.8140
	1	10.6458	10.4817	10.1919	10.2771	9.9255	9.8630	8.3916
	2	11.0945	11.0363	10.7307	10.8867	10.5050	10.5063	8.8928
	5	11.2116	11.3021	11.0203	11.2472	10.8738	10.9587	9.3238
1	0	6.3496	6.3496	6.3496	6.3496	6.3496	6.3496	6.3496
	1/3	8.7556	8.5676	8.4056	8.3944	8.2014	8.1036	7.2722
	0.5	9.4249	9.2255	9.0168	9.0289	8.7795	8.6821	7.6217
	1	10.1905	10.0259	9.7678	9.8314	9.5186	9.4489	8.1299
	2	10.6243	10.5478	10.2718	10.3970	10.0533	10.0361	8.5740
	5	10.7591	10.8122	10.5537	10.7421	10.4016	10.4565	8.9585
5	0	6.3496	6.3496	6.3496	6.3496	6.3496	6.3496	6.3496
	1/3	8.1605	8.0039	7.8848	7.8646	7.7221	7.6372	7.0127
	0.5	8.7067	8.5295	8.3727	8.3640	8.1763	8.0836	7.2705
	1	9.3670	9.1979	8.9973	9.0203	8.7777	8.6939	7.6519
	2	9.7790	9.6629	9.4408	9.5067	9.2319	9.1790	7.9917
	5	9.9553	9.9296	9.7133	9.8266	9.5453	9.5418	8.2914

the volume fractions of Al_2O_3 and ZrO_2 also increase. Since Young's modulus of Al is much lower than that of Al_2O_3 and ZrO_2, the effective modulus increases by increasing n_z and this leads to the increase of the beam rigidities. The mass moments also increase by increasing the index n_z, but this increase is much lower than that of the rigidities. As a result, the frequencies increase by increasing n_z. The decrease of the frequencies by increasing n_x can be also explained by a similar argument. The numerical results in Tables 4 to 6 reveal that the variation of the material properties in the length direction plays an important role in the frequencies of the BFGSW beams, and the desired frequency can be obtained by approximate choice of the material grading indexes.

Table 6. Fundamental frequency parameters of CF beam with $L/h = 20$ for various grading indexes and layer thickness ratios

n_x	n_z	(1-0-1)	(2-1-2)	(2-1-1)	(1-1-1)	(2-2-1)	(1-2-1)	(1-8-1)
1/3	0	1.0130	1.0130	1.0130	1.0130	1.0130	1.0130	1.0130
	1/3	1.4143	1.3863	1.3588	1.3592	1.3265	1.3119	1.1716
	0.5	1.5208	1.4934	1.4581	1.4639	1.4220	1.4090	1.2316
	1	1.6363	1.6189	1.5760	1.5926	1.5409	1.5352	1.3186
	2	1.6941	1.6949	1.6500	1.6788	1.6231	1.6289	1.3940
	5	1.7014	1.7265	1.6857	1.7263	1.6726	1.6927	1.4585
0.5	0	1.0130	1.0130	1.0130	1.0130	1.0130	1.0130	1.0130
	1/3	1.3444	1.3215	1.2990	1.2990	1.2723	1.2598	1.1433
	0.5	1.4339	1.4115	1.3825	1.3870	1.3526	1.3412	1.1932
	1	1.5313	1.5175	1.4819	1.4958	1.4531	1.4477	1.2658
	2	1.5795	1.5817	1.5442	1.5688	1.5226	1.5271	1.3291
	5	1.5841	1.6077	1.5735	1.6087	1.5640	1.5812	1.3835
1	0	1.0130	1.0130	1.0130	1.0130	1.0130	1.0130	1.0130
	1/3	1.2549	1.2383	1.2220	1.2218	1.2025	1.1928	1.1070
	0.5	1.3226	1.3064	1.2852	1.2883	1.2632	1.2540	1.1438
	1	1.3969	1.3876	1.3611	1.3715	1.3400	1.3352	1.1978
	2	1.4332	1.4368	1.4086	1.4278	1.3933	1.3963	1.2455
	5	1.4349	1.4559	1.4299	1.4582	1.4247	1.4381	1.2869
5	0	1.0130	1.0130	1.0130	1.0130	1.0130	1.0130	1.0130
	1/3	1.1854	1.1723	1.1607	1.1596	1.1459	1.1379	1.0765
	0.5	1.2387	1.2249	1.2094	1.2102	1.1920	1.1836	1.1023
	1	1.3003	1.2904	1.2704	1.2763	1.2525	1.2463	1.1414
	2	1.3334	1.3327	1.3107	1.3231	1.2964	1.2954	1.1767
	5	1.3390	1.3516	1.3307	1.3503	1.3236	1.3304	1.2080

Tables 4 to 6 also show an important role of the layer thickness ratio on the frequency of the sandwich beam. A larger core thickness the beam has a smaller frequency parameter is, regardless of the material index and the boundary conditions. However, the change of the frequency parameter by the change of the layer thickness ratio is different between the symmetrical and asymmetrical beams.

The variation of the first four frequency parameters μ_i ($i = 1..4$) with the material grading indexes is displayed in Figs. 3–5 for the SS, CC, and CF beams, respectively. The figures are obtained for the (2-1-2) beams with an aspect ratio $L/h = 20$. The dependence of the higher frequency parameters upon the grading indexes is similar to that of the fundamental frequency parameter. All the frequency parameters increase by increasing the index n_z, and they decrease by the increase of the index n_x, regardless of the boundary conditions.

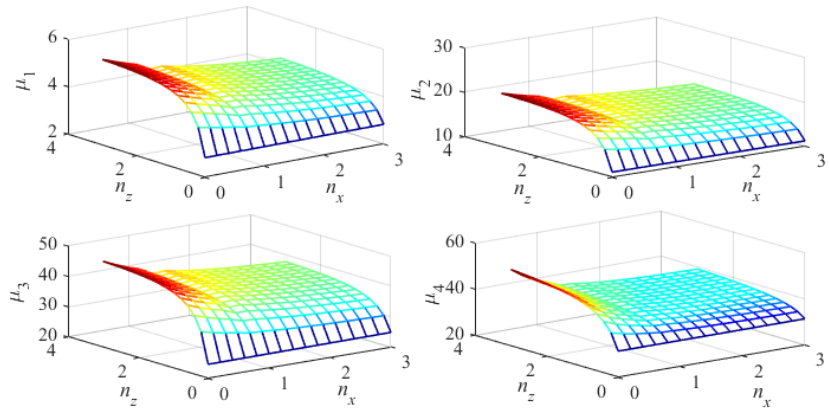

Figure 3. Variation of the first four frequency parameters with grading indexes of FGSW (2-1-2) SS beam

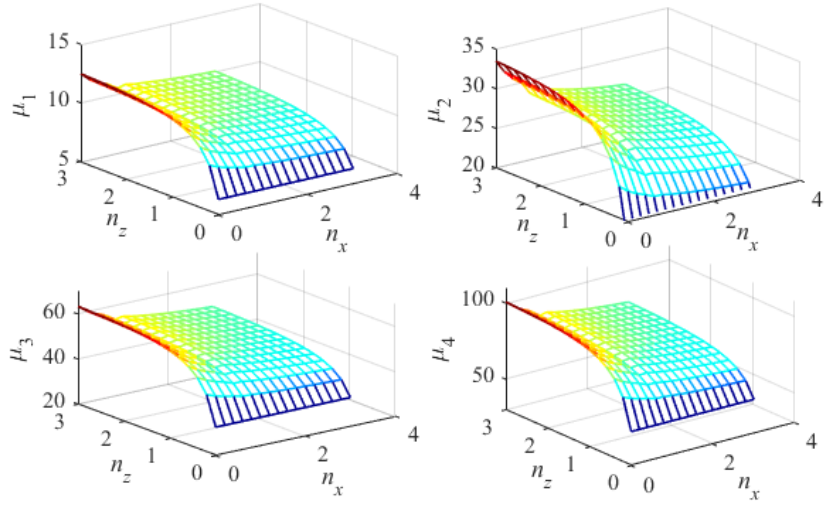

Figure 4. Variation of the first four frequency parameters with grading indexes of FGSW (2-1-2) CC beam

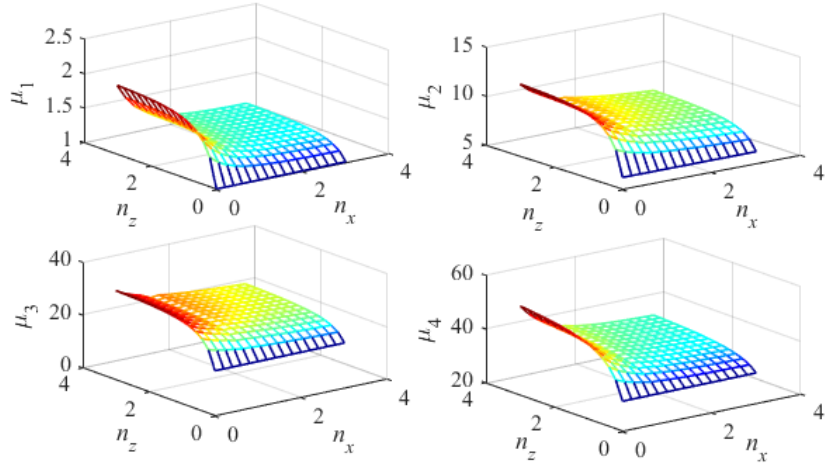

Figure 5. Variation of the first four frequency parameters with grading indexes of FGSW (2-1-2) CF beam

To show the influence of the aspect ratio on frequencies, the variation of fundamental frequency parameter with aspect ratio of the SS and CC beams is depicted in Fig. 6 for and various layer thickness ratios. We can see from the figure that the frequency parameter of the beams increases by the increase of the aspect ratio. The layer thickness ratio can change the frequency, but it hardly changes the dependence of the frequency on the aspect ratio. The result in Fig. 6 shows the good ability of the derived finite element formulation in modelling the effect of the shear deformation on the frequency of the BFGSW beam.

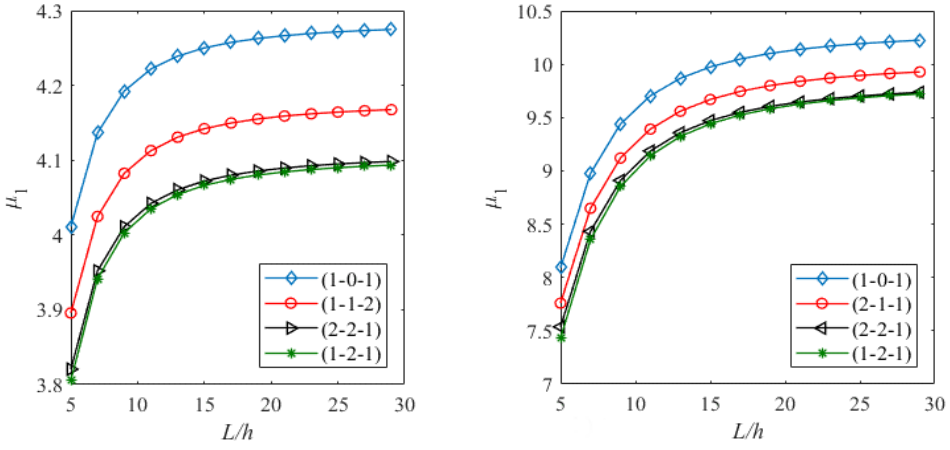

(a) SS beam (b) CC beam

Figure 6. Variation of fundamental frequency parameter with aspect ratio of BFGSW (1-2-1) beam with $n_x = n_z = 3$

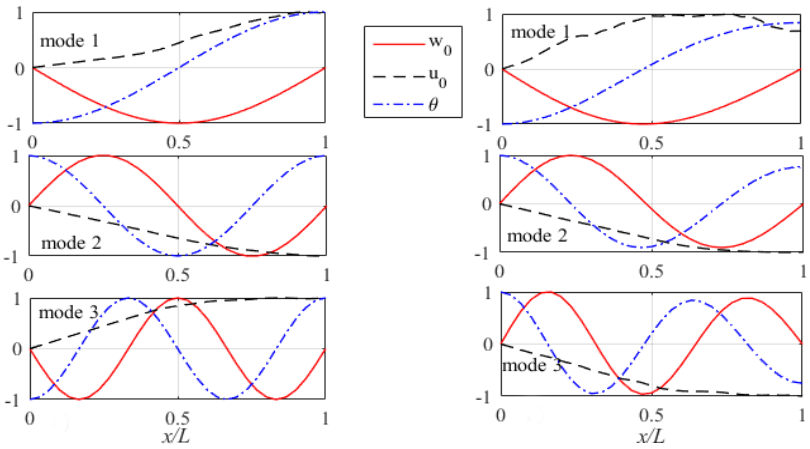

(a) $n_x = 0, n_z = 2$ (b) $n_x = 2, n_z = 2$

Figure 7. Three first mode shapes of (1-1-1) SS beam

In Fig. 7, the first three vibration modes for the transverse displacement w_0, axial displacement u_0, and rotation θ of the (1-1-1) SS beam are shown for two pairs of the grading indexes, $(n_x = 0, n_z = 2)$ and $(n_x = 2, n_z = 2)$. When $n_x = 0$, the beam becomes a unidirectional FGSW beam formed from

M1 and M3, and thus Fig. 7 illustrates the vibration modes of the unidirectional FGSW beam. The effect of the variation of the material properties in the longitudinal direction can be seen by comparing Fig. 7(a) and Fig. 7(b). The symmetrical shape with respect to the mid-line of the first mode of the transverse displacement w_0 and rotation θ as seen in Fig. 7(a) is no longer seen for the BFGSW beam in Fig. 7(b). Fig. 8 displays three first mode shapes of (1-2-1) BFGSW beam for$(n_x, n_z) = (1, 3)$ and $(n_x, n_z) = (3, 3)$. By comparing Figs. 8(a) and 8(b), it can see that the index n_x can change the vibration modes of the BFGSW beam. Thus, the effect of the material properties in the longitudinal direction is important in both the natural frequency and vibration mode of the BFGSW beam.

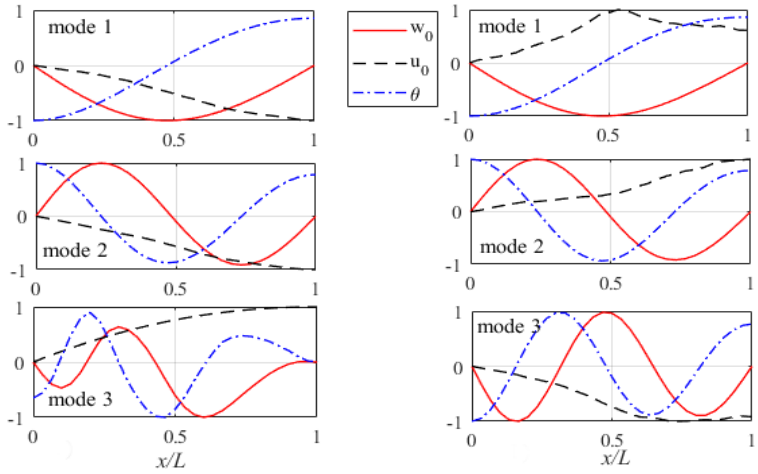

(a) $n_x = 1, n_z = 3$ (b) $n_x = 3, n_z = 3$

Figure 8. Three first mode shapes of (1-2-1) SS beam

5. Conclusions

Free vibration BFGSW beams having different boundary conditions are studied in the basis of the first-order shear deformation theory. A finite element formulation, in which the stiffness and mass matrices are explicitly evaluated, has been derived and employed in computing natural frequencies and mode shapes of the beams. The numerical result has confirmed the accuracy and the fast convergence of the derived formulation. The effects of the power-law indexes, the layer thickness and aspect ratios on the natural frequencies and vibration modes of the beams have been examined and highlighted. It is found that the frequency parameter increases by increasing the transverse index n_z, but it decreases by the increase of the axial index n_x. The obtained results also show an important role of the layer thickness ratio on the frequency of the sandwich beam, a larger core thickness the beam has a smaller frequency parameter is, regardless of the material index and the boundary conditions. The numerical results of the present work are useful in the design of FGM sandwich beams, and desired frequencies of the beams can be achieved by approximately choosing the power-law indexes.

References

[1] Koizumi, M. (1997). FGM activities in Japan. *Composites Part B: Engineering*, 28(1-2):1–4.

[2] Wakashima, K., Hirano, T., Niino, M. (1990). *Space applications of advanced structural materials*, volume 303. European Space Agency, Noordwijk, The Netherlands.
[3] Amirani, M. C., Khalili, S. M. R., Nemati, N. (2009). Free vibration analysis of sandwich beam with FG core using the element free Galerkin method. *Composite Structures*, 90(3):373–379.
[4] Vo, T. P., Thai, H.-T., Nguyen, T.-K., Maheri, A., Lee, J. (2014). Finite element model for vibration and buckling of functionally graded sandwich beams based on a refined shear deformation theory. *Engineering Structures*, 64:12–22.
[5] Vo, T. P., Thai, H.-T., Nguyen, T.-K., Inam, F., Lee, J. (2015). A quasi-3D theory for vibration and buckling of functionally graded sandwich beams. *Composite Structures*, 119:1–12.
[6] Bennai, R., Atmane, H. A., Tounsi, A. (2015). A new higher-order shear and normal deformation theory for functionally graded sandwich beams. *Steel and Composite Structures*, 19(3):521–546.
[7] Trinh, L. C., Vo, T. P., Osofero, A. I., Lee, J. (2016). Fundamental frequency analysis of functionally graded sandwich beams based on the state space approach. *Composite Structures*, 156:263–275.
[8] Su, Z., Jin, G., Wang, Y., Ye, X. (2016). A general Fourier formulation for vibration analysis of functionally graded sandwich beams with arbitrary boundary condition and resting on elastic foundations. *Acta Mechanica*, 227(5):1493–1514.
[9] Mashat, D. S., Carrera, E., Zenkour, A. M., Al Khateeb, S. A., Filippi, M. (2014). Free vibration of FGM layered beams by various theories and finite elements. *Composites Part B: Engineering*, 59:269–278.
[10] Şimşek, M., Al-Shujairi, M. (2017). Static, free and forced vibration of functionally graded (FG) sandwich beams excited by two successive moving harmonic loads. *Composites Part B: Engineering*, 108:18–34.
[11] Hung, D. X., Truong, H. Q. (2018). Free vibration analysis of sandwich beams with FG porous core and FGM faces resting on Winkler elastic foundation by various shear deformation theories. *Journal of Science and Technology in Civil Engineering (STCE)-NUCE*, 12(3):23–33.
[12] Şimşek, M. (2015). Bi-directional functionally graded materials (BDFGMs) for free and forced vibration of Timoshenko beams with various boundary conditions. *Composite Structures*, 133:968–978.
[13] Karamanlı, A. (2018). Free vibration analysis of two directional functionally graded beams using a third order shear deformation theory. *Composite Structures*, 189:127–136.
[14] Deng, H., Cheng, W. (2016). Dynamic characteristics analysis of bi-directional functionally graded Timoshenko beams. *Composite Structures*, 141:253–263.
[15] Nguyen, D. K., Nguyen, Q. H., Tran, T. T. (2017). Vibration of bi-dimensional functionally graded Timoshenko beams excited by a moving load. *Acta Mechanica*, 228(1):141–155.
[16] Nguyen, D. K., Tran, T. T. (2018). Free vibration of tapered BFGM beams using an efficient shear deformable finite element model. *Steel and Composite Structures*, 29(3):363–377.
[17] Thom, T. T., Kien, N. D. (2018). Free vibration analysis of 2-D FGM beams in thermal environment based on a new third-order shear deformation theory. *Vietnam Journal of Mechanics*, 40(2):121–140.
[18] Kosmatka, J. B. (1995). An improved two-node finite element for stability and natural frequencies of axial-loaded Timoshenko beams. *Computers & Structures*, 57(1):141–149.
[19] Shahba, A., Attarnejad, R., Marvi, M. T., Hajilar, S. (2011). Free vibration and stability analysis of axially functionally graded tapered Timoshenko beams with classical and non-classical boundary conditions. *Composites Part B: Engineering*, 42(4):801–808.

Appendix A.

Rigidities A_{ij} in Eq. (10)

$$\begin{aligned} &A_{11}^{M1} = bE_1(z_2 - z_1); \quad A_{11}^{M2} = bE_2(z_1 - z_0 + z_3 - z_2) \\ &A_{11}^{M1M2} = bE_{12}\left(\frac{z_1 - z_0 + z_3 - z_2}{n_z + 1}\right); \quad A_{11}^{M2M3} = bE_{23}\left(1 - \frac{1}{n_z + 1}\right)(z_1 - z_0 + z_3 - z_2) \end{aligned} \tag{A.1}$$

$$A_{12}^{M1} = bE_1\left(\frac{z_2^2 - z_1^2}{2}\right); \quad A_{12}^{M2} = bE_2\left(\frac{z_1^2 - z_0^2 + z_3^2 - z_2^2}{2}\right)$$

$$A_{12}^{M1M2} = bE_{12}\left(\frac{(z_1 - z_0)^2 - (z_2 - z_3)^2}{n_z + 2} + \frac{z_0\,(z_1 - z_0) - z_3\,(z_2 - z_3)}{n_z + 1}\right) \tag{A.2}$$

$$A_{12}^{M2M3} = bE_{23}\left(\frac{(z_1 - z_0)^2 - (z_2 - z_3)^2}{n_z + 2} + \frac{z_0\,(z_1 - z_0) - z_3\,(z_2 - z_3)}{n_z + 1} - \frac{z_1^2 - z_0^2 + z_3^2 - z_2^2}{2}\right)$$

$$A_{22}^{M1} = bE_1\left(\frac{z_2^3 - z_1^3}{3}\right); \quad A_{22}^{M2} = bE_2\left(\frac{z_1^3 - z_0^3 + z_3^3 - z_2^3}{3}\right)$$

$$A_{22}^{M1M2} = bE_{12}\left(\frac{(z_1 - z_0)^3 - (z_2 - z_3)^3}{n_z + 3} + 2\frac{z_0(z_1 - z_0)^2 - z_3(z_2 - z_3)^2}{n_z + 2} + \frac{z_0^2\,(z_1 - z_0) - z_3^2\,(z_2 - z_3)}{n_z + 1}\right)$$

$$A_{22}^{M2M3} = bE_{23}\left[\frac{(z_1 - z_0)^3 - (z_2 - z_3)^3}{n_z + 3} + 2\frac{z_0(z_1 - z_0)^2 - z_3(z_2 - z_3)^2}{n_z + 2} + \frac{z_0^2\,(z_1 - z_0) - z_3^2\,(z_2 - z_3)}{n_z + 1} - \frac{z_1^3 - z_0^3 + z_3^3 - z_2^3}{3}\right] \tag{A.3}$$

$$A_{33}^{M1} = bG_1(z_2 - z_1); \quad A_{33}^{M2} = bG_2(z_1 - z_0 + z_3 - z_2)$$

$$A_{33}^{M1M2} = bG_{12}\left(\frac{z_1 - z_0 + z_3 - z_2}{n_z + 1}\right); \quad A_{33}^{M2M3} = bG_{23}\left(1 - \frac{1}{n_z + 1}\right)(z_1 - z_0 + z_3 - z_2) \tag{A.4}$$

where $E_{12} = E_1 - E_2, E_{23} = E_2 - E_3, G_{12} = G_1 - G_2, G_{23} = G_2 - G_3$.

Mass moments I_{ij} in Eq. (13)

$$I_{11}^{M1} = b\rho_1(z_2 - z_1); \quad I_{11}^{M2} = b\rho_2(z_1 - z_0 + z_3 - z_2)$$

$$I_{11}^{M1M2} = b\rho_{12}\left(\frac{z_1 - z_0 + z_3 - z_2}{n_z + 1}\right); \quad I_{11}^{M2M3} = b\rho_{23}\left(1 - \frac{1}{n_z + 1}\right)(z_1 - z_0 + z_3 - z_2) \tag{A.5}$$

$$I_{12}^{M1} = b\rho_1\left(\frac{z_2^2 - z_1^2}{2}\right); \quad I_{12}^{M2} = b\rho_2\left(\frac{z_1^2 - z_0^2 + z_3^2 - z_2^2}{2}\right)$$

$$I_{12}^{M1M2} = b\rho_{12}\left(\frac{(z_1 - z_0)^2 - (z_2 - z_3)^2}{n_z + 2} + \frac{z_0\,(z_1 - z_0) - z_3\,(z_2 - z_3)}{n_z + 1}\right) \tag{A.6}$$

$$I_{12}^{M2M3} = b\rho_{23}\left(\frac{(z_1 - z_0)^2 - (z_2 - z_3)^2}{n_z + 2} + \frac{z_0\,(z_1 - z_0) - z_3\,(z_2 - z_3)}{n_z + 1} - \frac{z_1^2 - z_0^2 + z_3^2 - z_2^2}{2}\right)$$

$$I_{22}^{M1} = b\rho_1\left(\frac{z_2^3 - z_1^3}{3}\right); \quad I_{22}^{M2} = b\rho_2\left(\frac{z_1^3 - z_0^3 + z_3^3 - z_2^3}{3}\right)$$

$$I_{22}^{M1M2} = b\rho_{12}\left(\frac{(z_1 - z_0)^3 - (z_2 - z_3)^3}{n_z + 3} + 2\frac{z_0(z_1 - z_0)^2 - z_3(z_2 - z_3)^2}{n_z + 2} + \frac{z_0^2\,(z_1 - z_0) - z_3^2\,(z_2 - z_3)}{n_z + 1}\right)$$

$$I_{22}^{M2M3} = b\rho_{23}\left[\frac{(z_1 - z_0)^3 - (z_2 - z_3)^3}{n_z + 3} + 2\frac{z_0(z_1 - z_0)^2 - z_3(z_2 - z_3)^2}{n_z + 2} + \frac{z_0^2\,(z_1 - z_0) - z_3^2\,(z_2 - z_3)}{n_z + 1} - \frac{z_1^3 - z_0^3 + z_3^3 - z_2^3}{3}\right] \tag{A.7}$$

where $\rho_{12} = \rho_1 - \rho_2, \rho_{23} = \rho_2 - \rho_3$.